IEEE Access
Multidisciplinary | Rapid Review | Open Access Journal

Received January 11, 2020, accepted January 23, 2020, date of publication February 10, 2020, date of current version February 18, 2020.

Digital Object Identifier 10.1109/ACCESS.2020.2972558

Development and Characterization of Freestanding Poly (Methyl Methacrylate)/ Monolayer Graphene Membrane

BADARIAH BAIS[1,2], (Senior Member, IEEE), NORLIANA YUSOF[2,3], NORHAYATI SOIN[4], (Senior Member, IEEE), JUMRIL YUNAS[2], AND BURHANUDDIN YEOP MAJLIS[2], (Senior Member, IEEE)

[1]Department of Electrical, Electronic, and Systems Engineering, Faculty of Engineering and Built Environment, Universiti Kebangsaan Malaysia, 43600 Bangi, Malaysia
[2]Institute of Microengineering and Nanoelectronics (IMEN), Universiti Kebangsaan Malaysia, 43600 Bangi, Malaysia
[3]Faculty of Innovative Design and Technology, Universiti Sultan Zainal Abidin, Kuala Terengganu 21300, Malaysia
[4]Department of Electrical Engineering, Faculty of Engineering, University of Malaya, Kuala Lumpur 50603, Malaysia

Corresponding author: Badariah Bais (badariah@ukm.edu.my)

This work was supported by the project under Grant DIP-2018-019.

ABSTRACT Graphene-polymer based materials are gaining more popularity among researchers due to its mechanical properties that are found to be suitable to be used in various micro/nanoscale application requiring highly sensitive sensors. This research ventured into the fabrication and characterization process of a freestanding poly (methyl methacrylate) (PMMA) on monolayer graphene (Gr) yielding a (PMMA/Gr) membrane. In the process of transferring the chemical vapor deposition (CVD) graphene film over a cavity that was developed on a silicon substrate, the wet transfer method was used. Five repetitions of the nanoindentation testing had been carried out on the flexible membrane which resulted in a reproducible deflection, when exerted with a maximum loading of 10 mN. The indented (PMMA/Gr) membrane showed an identical elastic behavior with Young's modulus of 0.18 GPa. The highest deflection of approximately 22 μm at 1.6 mN maximum loads and the tensile stress of 0.58 MPa was obtained from the indentation testing analysis. The combination of PMMA-Graphene materials as a membrane has shown impressive changes to its mechanical properties. Besides maintaining its viscoelastic-plastic behavior which contributed to its flexibility, the presence of a graphene layer provided strong support to prevent damages to the membrane. Meanwhile, PMMA properties with low elastic modulus have contributed to the increased of the mechanical sensitivity of the membrane. Based on this research, the mechanical sensitivity of (PMMA/Gr) is reported to be 0.15 nm/Pa, which is much higher compared to a typical conventional membrane. It was proven that the hybrid (PMMA/Gr) membrane was extremely sensitive to the subjected pressures, thus, shown its potential to be applied as a micro-electro-mechanical systems (MEMS) capacitive pressure sensor.

INDEX TERMS Biomembranes, nanofabrication, microsensors.

I. INTRODUCTION

Graphene membrane has garnered significant popularity due to its extraordinary mechanical, electrical and thermal properties, as well as the ability to produce graphene-based devices. One of the interesting mechanical behaviors of a graphene membrane is that it can be easily constructed using the transfer method which only utilized the van der Waals (vdW) adhesion between the underlying substrate and the graphene layer to fix the membrane in place. Due to the material properties of the layered graphene-polymer that may not be similar to the material of the bulk polymer [1], [2], it has piqued the interest of many researchers to investigate further on the characterization of the freestanding layered graphene-polymers. Hence, extensive research on the behavior of the freestanding (PMMA/Gr) membranes is crucial in order to

The associate editor coordinating the review of this manuscript and approving it for publication was Rahul A. Trivedi.

produce more accurate and precise mechanical properties of graphene-based devices and to determine their suitability for specific applications.

In pressure sensing applications, a highly sensitive membrane is desirable as it will be able to increase the accuracy and effectiveness of a pressure sensor. For a freestanding membrane, the sensitivity can be increased by increasing the area of the suspended membrane, decreasing the dielectric gap or utilizing membrane materials that have lower elastic modulus [3]. Prior to this specific research, the monolayer graphene along with the low elastic modulus and low density of PMMA was utilized. In a hybrid (PMMA/Gr) membrane, the graphene serves as high-conductive layer and provides a strong adhesion between the membrane and the of silicon nitride (Si3N4) layer as the results of the van der waals interaction [4]. The PMMA plays two key roles: first, to improve the mechanical sensitivity of the membrane due to its low elastic modulus and second as an efficient holder for the graphene thin film to prevent it from collapsing into the cavity area. Besides, PMMA is basically a biocompatible polyester with high resistance to chemical reactions and most importantly, it does not cause toxicity [5]. The combination of these two materials is believed to improve the displacement and thus, increasing the mechanical sensitivity of the membrane. In a previous study by Ramanathan *et al.*, it was reported that with approximately 1 wt% addition of graphene to PMMA, an increase of approximately 80% in the elastic modulus was achieved and it also led to an increase of approximately 20% in the ultimate tensile strength [6], [7]. Furthermore, interestingly for a defect-free single-layer graphene, its intrinsic strength was recorded to be at 42 N/m, which was equivalent to 130 GPa and was considered to be one of the strongest materials [8]–[10]. In a study conducted by Blees *et.al.* [11], [12], the monolayer graphene could be stretched up to 240% of its initial strength without breaking. Based on the above-mentioned features, a hybrid of (PMMA/Gr) membrane is believed to be a promising material in improvising the sensitivity of capacitive MEMS sensing actuators.

To explore the mechanical properties of various materials at the micro or nanoscale level, nanoindentation testing is a well-known technique to be applied. The nanoindentation technique is carried out by exerting a sharp and hard tip into a sample material and simultaneously recording the force-displacement data which will provide the information on the mechanical properties of the material that has been tested [13]. A considerable number of researches has utilized this technique to investigate the mechanical properties of polymers and graphene-based materials [1], [14]–[19]. Kotsilkova *et al.* [1] investigated the mechanical properties of the freestanding and the supported bilayer graphene/poly (methylmethacrylate) films. Wang *et al.* [14] explored mechanical properties of polydimethylsiloxane (PDMS) while Niu *et al.* [15] performed an indentation test of a graphene single layer mounted on a PDMS substrate (graphene/PDMS). Chen *et al.* [16] studied the mechanical properties of the graphene on poly (ethylene terephthalate) substrate. Zhu *et al.* [17] conducted nanoindentation testing with molecular dynamics (MD) simulations to study the effects of graphene (Gr) coating on the deformation behavior of an ⟨001⟩ orientation copper (Cu) substrate. Zhang and Pan [18] in their study analyzed the mechanical properties and a number of layers of graphene from the nanoindentation. Kang *et al.* [19] had conducted some research on the mechanical properties of the freestanding graphene oxide (GO) films. The experiment was carried out using nanoindentation on the system of a dynamic contact module (DCM).

In this work, the micro-fabrication approach to develop a freestanding monolayer graphene-PMMA (PMMA/Gr) membrane is described as shown in Figure 1. The mechanical properties of materials such as stress-strain, Young's modulus (Es), tensile stress (σ_{max}) and plasticity index (ψ) were analyzed from the indentation system software. These parameters of the hybrid membrane were investigated and compared with the results from the previous studies. The aim of this study is to determine the material properties of (PMMA/Gr) membrane, which in turn, is expected to significantly assist in the development of MEMS capacitive pressure sensors applications such as microphones, biomedical and biochemical sensors.

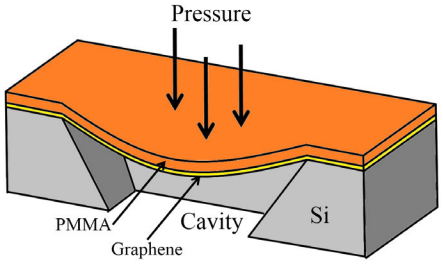

FIGURE 1. Cross-section of a suspended PMMA / Gr membrane.

II. METHODOLOGY

A. FABRICATION OF FREESTANDING (PMMA/Gr) MEMBRANE

The silicon cavity was fabricated using bulk micromachining which involved lithography and wet etching process. The wafers used in this study were supplied by University Wafer Inc., with a thickness of 500 μm, ⟨100⟩ orientation, n-doped and coated with 300 nm silicon nitride on both sides. After dicing the wafer, the samples were cleaned by subsequently sonicated in acetone, methanol and deionized (DI) water. Then, the samples were spin-coated with positive photoresist and were exposed to ultra-violet light. In order to prepare the window pattern for the potassium hydroxide (KOH) wet etching, the silicon nitride layer was removed. Buffered oxide etchant (BOE) etching method was used to remove the nitride layer with the etching rate of 45 nm min^{-1} at 80 °C. Finally, wet anisotropic etching was performed by submerging with 45% KOH + 10% surfactant at 80 °C for 6.5 hours to fully etched the silicon cavity. The detailed fabrication process

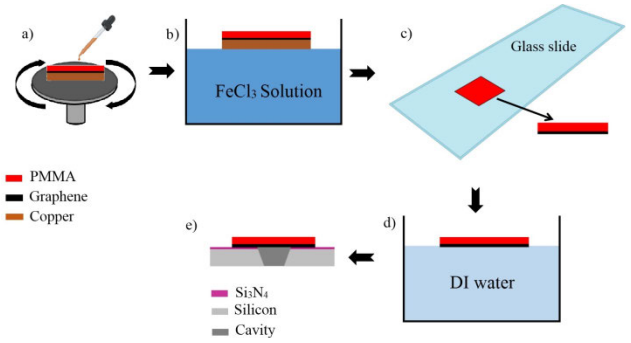

FIGURE 2. Schematic diagram of the (PMMA/Gr) film transfer process to the etched silicon structure. (a) A thin liquid PMMA layer is spin- coated onto CVD graphene on copper; (b) bottom copper layer was then etched by 0.5 M ferric chloride ($FeCl_3$) solution for 3 hours; (c) The (PMMA/Gr) film is lifted off using glass slide; (d) The (PMMA/Gr) film is transferred to DI water; (e) The (PMMA/Gr) film is transferred onto etched silicon structure.

of wet silicon etching using KOH has been extensively discussed in the previous studies [20]–[22].

The (PMMA/Gr) layer was transferred onto the silicon cavity by employing the wet graphene transfer process as had been discussed in previous studies [23]–[25]. Transferring (PMMA/Gr) layer onto the etched silicon forming a freestanding membrane is a crucial task where any mishandling during the transferring process may cause the membrane to rupture into the cavity area. Figure 2 illustrates the schematic diagram of the (PMMA/Gr) film transfer process to the etched silicon forming a freestanding (PMMA/Gr) membrane. Monolayer CVD graphene films on 18 μm copper were supplied by University Wafer Inc. (known as CVD graphene on copper). PMMA solution (950 PMMA A4, 950 K MW 4 wt% in anisole by MICRO CHEM was spin-coated on top of the CVD graphene on copper samples at 3000 rpm for 60 s forming a sandwiched layer of PMMA and graphene film (PMMA/Gr). These samples were then dried on a hot plate at 100 °C for 10 min. The bottom copper layer was then etched by 0.5 M ferric chloride (FeCl3) solution for 3 hours. In order to have a stable and slow etch rate (<500 nm/h), a low concentration of etchant (0.5M) was maintained to avoid the fabrication of copper foil into sub-millimeter grains that might sink and tear the floating graphene layer [26]. In order to remove any residues from the etching process, these samples were then transferred to distilled (DI) water by using the glass slide. The (PMMA/Gr) layer was then picked up onto the target substrate that had been etched (500 μm^2 square cavity of silicon). The next stage involved draining out the water between the substrate and the graphene and was carried out by holding the samples vertically. The samples were later baked at 100 °C for 20 mins to ensure that any remaining water molecules were removed and to increase adhesion between the graphene and the Si3N4 layer.

The surface topography of CVD graphene on copper was characterized by Atomic force microscope (AFM) (Park Systems, NX-10) and the (PMMA/Gr) membrane was characterized by Field emission scanning electron microscope FESEM (Zeiss, SUPRA 55VP). Raman spectroscopy system (Thermo Scientific, DXR2xi) was utilized to obtain the Raman spectra of the membrane to determine the number of layer and coverage distribution of the graphene. The Raman spectra was excited using a 514- nm laser in the range of 0 – 3000 cm^{-1}.

B. NANOINDENTATION TESTING OF FREESTANDING (PMMA/Gr) MEMBRANE

The nanoindentation test was performed using a calibrated indenter (MicroMaterials NanoTest) that was equipped with a Berkovich diamond tip with a radius of 3.5 μm. During the indentation process, the calibrated tip of the indenter was slowly brought down to touch the surface of the sample. When the tip and the surface of the sample came into contact, the applied force was linearly increased until it reached the maximum peak load and/or maximum penetration depth. At this stage, the force applied was fixed at the range of 0 to 10 mN whilst the loading rate was kept at a constant value of 5 mN/s. This was to reduce the risk of viscoelastic deformation during the loading cycle [27]. For each test, the hold period or the dwell time between the loading and unloading cycle was set at 1s. The dwell settings at each cycle are important as it allows the substrate and the instrument to stabilize before the load and depth values are recorded [28]. To achieve consistencies and repeatability of the results, the test was repeated for another four times using the same sample. In total, five tests were carried out throughout the sample. The diagram in Figure 3 shows the nanoindentation testing with the (PMMA/Gr) membrane being indented at the center of the membrane.

The tensile stress (σ_{max}) of the material using a nanoindentation test can be determined using Equation (1) as [29], [30]:

$$\sigma_{\max} = \left(\frac{1-2\upsilon}{2\pi}\right)\left(\frac{4E_r}{3R}\right)^{2/3}(P)^{1/3} \quad (1)$$

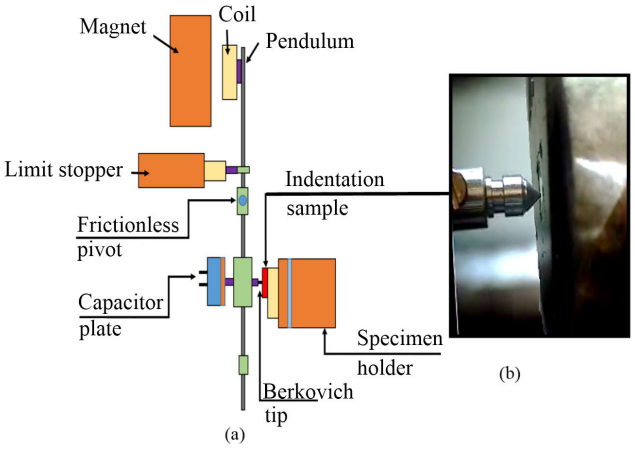

FIGURE 3. a) Indentation testing using MicroMaterials Nano Test. b) Indented (PMMA/Gr) membrane sample by Berkovich tip.

where ν, Er, R and P are Poison's ratio, reduced modulus, tip radius and peak load, respectively.

The Young's modulus, E_S of the sensing membrane material can be extracted from stress-strain plot while the plasticity index (ψ) of the material can be defined by calculating the area below the loading and unloading of the load-deflection curve. One of the functions of the plasticity index is to distinguish the elastic-plastic response of a material that is being subjected to external stresses and strains. In the nanoindentation test, the plasticity index of the material can be determined using Equation (2) [2] [31]:

$$\psi = \left(\frac{A_1 - A_2}{A_1}\right) \tag{2}$$

where $A1$ and $A2$ are the area under the loading and unloading curve, respectively.

III. RESULTS AND DISCUSSION

A. AFM CHARACTERIZATION OF CVD GRAPHENE AND FESEM IMAGES OF FREESTANDING (PMMA/Gr) MEMBRANE

Figure 4(a) shows the three-dimensional surface topography of a 30 μm × 30 μm CVD graphene on copper that has been obtained via the atomic force microscopy (AFM) and Figure 4(b) shows the cross-section elemental AFM analysis of the CVD graphene on copper. According to Figure 4(a), the surface of CVD graphene on copper resembled an island-like shape. The formation of the island-like shape and wrinkles was almost unavoidable for a CVD graphene [12] due to the fact that the copper substrate employed was not entirely flat. Secondly, the CVD was potentially formed due to the difference in the thermal coefficients of the copper substrate ($\sim 20 \times 10^{-6}$ K^{-1}) and graphene (-8.0×10^{-6} K^{-1}) [32]. From Figure 4(b), the peak height of the CVD graphene on copper was approximately 60 −100 nm.

The FESEM images on 30× and 150× magnification of (PMMA/Gr) membrane are shown in Figure 4(c) and Figure 4(d), respectively. Both FESEM images showed that the (PMMA/Gr) membrane was well suspended on the approximately 500 μm^2 silicon cavity area. These results showed that the (PMMA/Gr) film was successfully transferred over to the silicon etched cavity forming a freestanding (PMMA/Gr) membrane. Figure 4(e) shows the cross-section FESEM image of the freestanding (PMMA/Gr) membrane with a measured membrane thickness of approximately 0.5 μm. The bumpy surface of (PMMA/Gr) membrane shown in Figure 4(e) resulted from the island-like shape of CVD graphene on copper as previously shown by AFM image in Figure 4(a).

B. RAMAN SPECTROSCOPY CHARACTERIZATIONS

Raman spectroscopy had been employed to testify the existence of graphene and the number of graphene layers of the (PMMA/Gr) membrane. Perfect graphene exhibited prominent peaks in the Raman spectrum at G and 2D bands, at about 1580 cm^{-1} and 2690 cm^{-1} respectively [33]–[35]. The numbers of the graphic layers can be determined by the peak intensity ratio of 2D to peak G (I_{2D}/I_G). As a reference, the ratio for monolayer graphene is $I_{2D}/I_G \sim 2$–3, meanwhile for bilayer graphene, the ratio is $2 > I_{2D}/I_G > 1$ and for multilayer, the ratio is $I_{2D}/I_G < 1$ [36]. Figure 5 presents the Raman spectra of the freestanding (PMMA/Gr) membrane at four different locations from 1000 cm^{-1} to 3000 cm^{-1} range of Raman shift. According to Figure 5, the intensity of graphene at the 2D band was much higher than the G band for the freestanding membrane indicating that the graphene was prominent which testified the existence of graphene in the membrane.

TABLE 1 shows the Raman peak intensity values of G and 2D bands for the (PMMA/Gr) membrane. Based on TABLE 1, the ratios of I_{2D} /I_G of all four different locations were in the range of 2–3, which proved that the (PMMA/Gr) membrane consisted of mono-layer graphene. The very low intensity of D peak at 1350 cm^{-1} (ID) shown in Figure 5 concluded that this sample was composed of high-quality graphene. Figure 6 shows the color contours for peaks 2D and G. The red colors show random distributions of intensity for 2D peak while the blue contours show intensity for G peak. From the color contributions, it showed that the graphene existence was prominent due to a wider coverage of the red contours (2D peak) compared to the blue (G peak) contours.

TABLE 1. Intensity value and ratio of I_{2D}/I_G for (PMMA/Gr) membrane.

Point	I_{2D}	I_G	I_{2D}/I_G
1	31.293	15.215	2.06
2	48.014	23.606	2.03
3	45.957	17.416	2.64
4	60.925	30.236	2.01

C. NANOINDENTATION TESTING

1) LOAD-DEFLECTION CURVE

Figure 7 illustrates the load-deflection curve of (PMMA/Gr) freestanding membranes from the indentation testing. The loading and unloading cycles were repeated at five different locations on the same membrane to test their elastic behavior. From Figure 7, all loading and unloading curves almost completely overlapped and followed a cubic law, indicating the full reversibility of the membrane deformations [37]. The full reversibility of load-deflection curves exhibited an interesting viscoelastic-plastic behavior of the (PMMA/Gr) membrane and showed the highly repeatable loading-unloading cycles without rupturing the membranes. From the indentation, the measured value for maximum deflection, plastic depth, maximum load and reduced modulus were summarized in TABLE 2. According to TABLE 2, it showed that the membrane was stretched plastically with a very high deflection of average 22 μm at the maximum load of 1.6 mN. High deflection of the membrane was highly required in

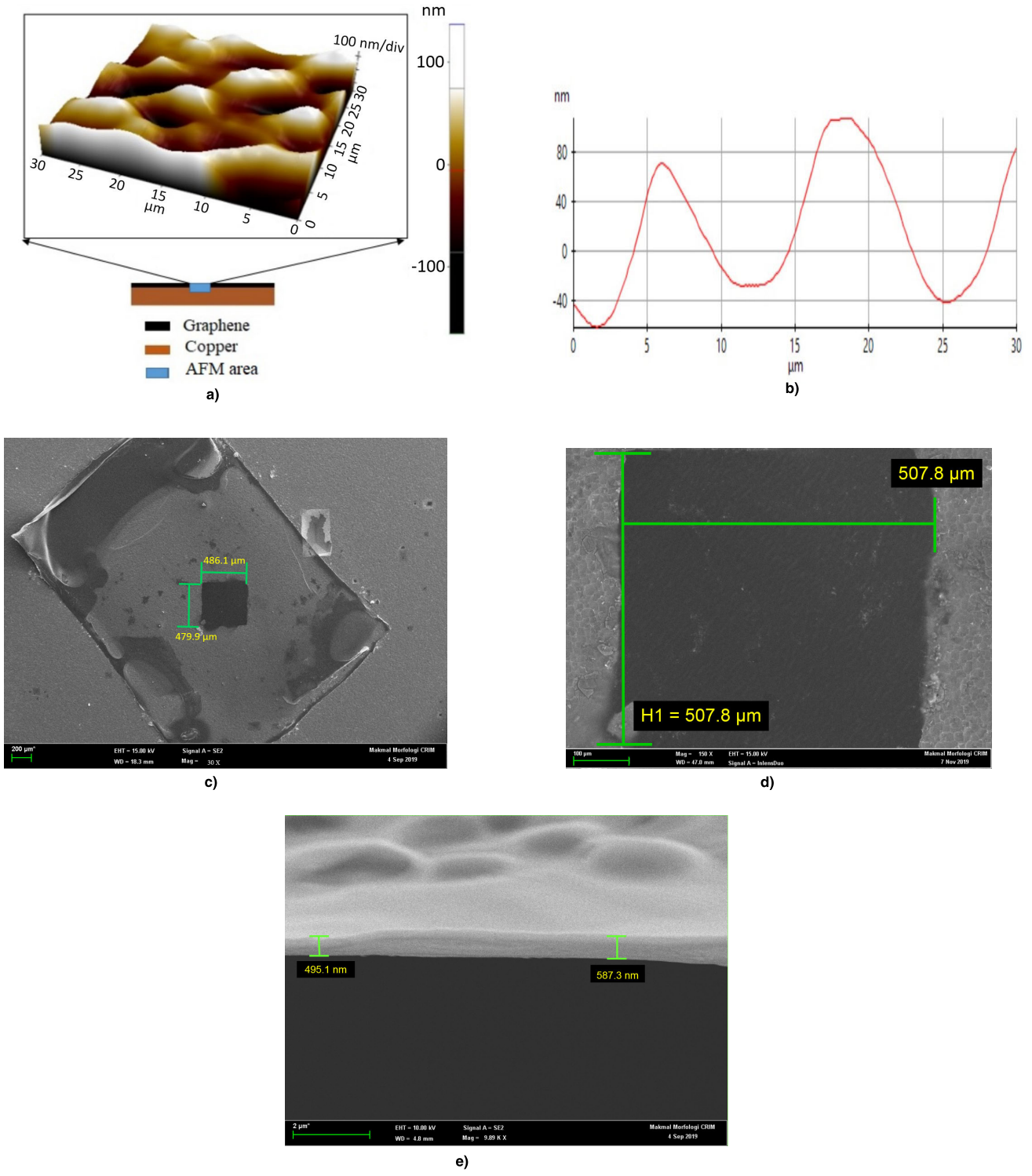

FIGURE 4. a) Three dimensional AFM image of the CVD graphene on the copper surface with the area of AFM is captured. b) Cross-sectional of AFM elemental analysis. c) FESEM image on 30× magnification of the freestanding (PMMA/Gr) membrane. d) FESEM image on 150× magnification of the freestanding (PMMA/Gr) membrane. e) Cross-section FESEM image of the freestanding (PMMA/Gr) membrane.

designing a membrane-based sensor as it would increase the mechanical sensitivity of the sensor [38]. In general, by applying a certain amount of force onto the membrane, the transducers will sense the stress as the result of membrane deflections. Thus, the mechanical sensitivity of the membrane can be defined by the slope of the pressure versus deflection curve [39], [40]. By calculating the applied load to the projected area, the pressure-induced to the membrane can

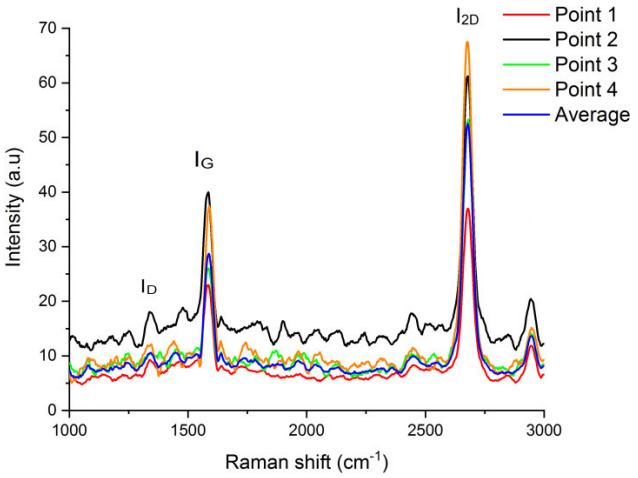

FIGURE 5. Raman peaks (G and 2D) for (PMMA/Gr) membrane.

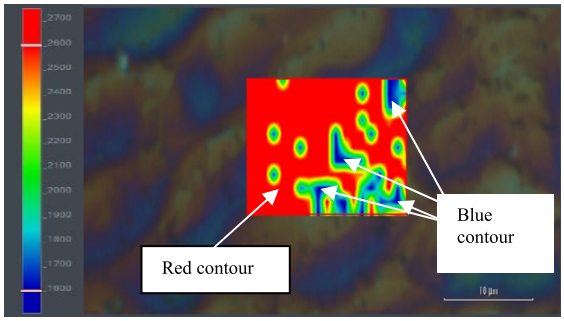

FIGURE 6. Raman mapping of freestanding (PMMA/Gr) membrane.

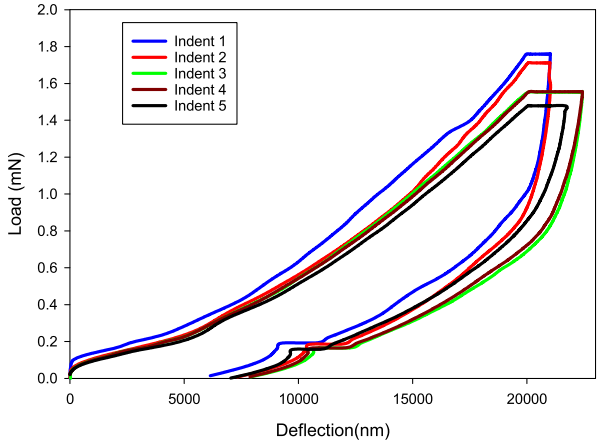

FIGURE 7. Load-deflection curve of freestanding (PMMA/Gr) membrane.

be analyzed, subsequently providing the estimation of the mechanical sensitivity. For Berkovich tip, the projected area, A is estimated as $A \approx 24.5\ \mathrm{hmax}^2$ where hmax is the maximum deflection [28]. Hence, the mechanical sensitivity of the (PMMA/Gr) membrane was calculated at approximately 0.15 nm/Pa which was higher compared to a typical conventional membrane [38], [41], [42]. In a previous research conducted by Chen *et al*. [43], the graphene membrane can boost the sensitivity up to 700% increment compared to the silicon membrane. Hence, this study has proven that the

TABLE 2. Mechanical Properties of (PMMA/Gr) membrane from indentation testing.

Indent	Maximum Deflection (nm)	Plastic Depth (nm)	Max Load (mN)	Reduced Modulus, Er (MPa)
1	21025.95	16382.1	1.76	3.03
2	21031.92	17025.3	1.71	3.29
3	22432.21	17194.8	1.55	2.26
4	22424.16	16934.2	1.55	2.19
5	21696.34	16631.6	1.48	2.30
Average	**21722.12**	**16833.6**	**1.61**	**2.61**

(PMMA/Gr) membrane is a good choice for low - pressure detection applications which requires high sensitivity especially for biomedical devices such as intracranial, intraocular and bladder MEMS capacitive pressure sensors.

Tensile stress value is one of the imperative properties of a membrane, in which lower tensile stress will contribute to the increase in the mechanical sensitivity of the membrane [44]. By substituting the parameters in Table 2 into the Equation (1) with values of $v = 0.345$ for graphene-PMMA layer [45], the tensile stress of (PMMA/Gr) membrane was found to have average tensile stress of 0.58 MPa. The comparison was made with the previous works on tensile stress for various type of membranes' material. In a study conducted by Kotsilkova *et al.* [1], the tensile stress of bilayer graphene-PMMA membrane was reported at 1.35 MPa while Torkkeli *et al.,* reported a value of 2.2 MPa for the tensile stress of polysilicon membrane [46]. In their experiment, Kronast *et al.,* have recorded a value of 0.13 GPa for silicon nitride membrane [47], while tensile stress was recorded at 1.5 GPa by Ganji *et al.,* for their aluminum diaphragm [37]. Based on the previous works, as compared to these notable findings, it is evident that the tensile stress of 0.58 MPa for this monolayer graphene-PMMA membrane under study is one of the lowest, hence contributing to the increased in the mechanical sensitivity of the membrane. In light of this finding, the proposed (PMMA/Gr) membrane is highly recommended to boost the sensitivity of MEMS capacitive pressure sensor devices.

2) PLASTICITY INDEX

The total energy spent and energy released during indentation can be specified by the area below the loading and unloading curve, respectively. During the nanoindentation test, the irreversible work can be estimated based on the difference between the area below the loading and unloading curves. For materials with viscoelastic-plastic behavior, the plasticity index is in the range of $0 < \psi < 1$. Fully-elastic behavior is represented by $\psi = 0$ and the fully plastic behavior of materials is represented by $\psi = 1$ [2]. Figure 8 shows the average area below the loading and unloading curve during five repetitions of the nanoindentation test. According to Figure 8, the area below the loading was greater than the unloading area indicating that the plasticity index should be

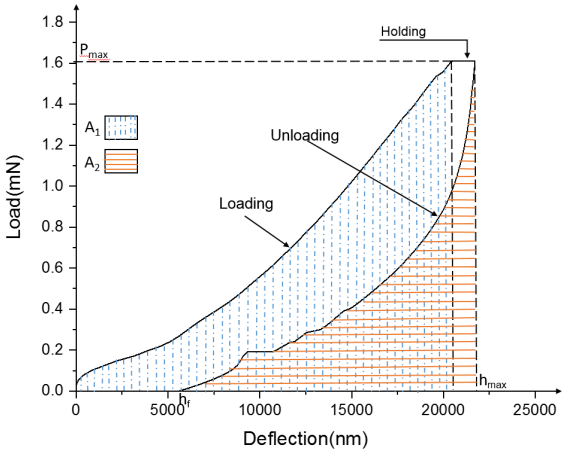

FIGURE 8. The area below the loading and unloading of the load-deflection curve.

TABLE 3. Plasticity index of (PMMA/Gr) membrane.

Indent	Plasticity Index, Ψ
1	0.55
2	0.58
3	0.55
4	0.53
5	0.49
Average	0.54

in the range of $0 < \psi < 1$. Referring to TABLE 3, the value of the plasticity index was calculated using Equation (2). From TABLE 3, it can be seen that the (PMMA/Gr) membrane displayed the viscoelastic-plastic behavior with the average plasticity index of 0.54. The results indicated that the membrane had both viscous and elastic characteristics when undergoing deformation.

3) STRESS-STRAIN CURVE

The mechanical properties of the material can be further analyzed by extracting the stress-strain data from the load deflection results. In understanding the mechanics of materials, Young's modulus, Es can be found from the slopes of the linear strain-stress curves under elastic deformation. Stress-strain curve for the average value of five repetitions of indentation on freestanding (PMMA/Gr) membrane is shown in Figure 9. From Figure 9, the elastic response of graphene was considered to be nonlinear. This consideration was made based on the fact that the stress-strain curve must reach a maximum point which provided the intrinsic breaking stress value [2]. The gradient of the linear part of the curve will provide Young's modulus value [48]. The linear region of the curve can be fitted using a linear equation $y = 184.14x - 0.66$, in which the slope was approximately 0.18 GPa, which was Young's modulus value. The results were found to be competitive with the previous results published by Woo *et al.* [45], which reported a 0.67 GPa of Young's modulus for the composition consisting

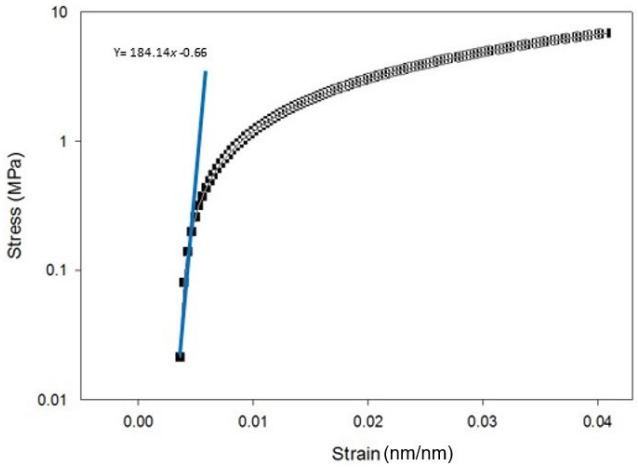

FIGURE 9. Stress-strain curve for a freestanding (PMMA/Gr) membrane.

of 0.3 μm and 3.0 μm of graphene and PMMA layer, respectively. The measured value of Es for the different compositions can be varied by changing its thickness. According to Woo *et al.* [45], it was discovered that the value of Es was reduced as a result of decreasing the graphene's thickness and increasing the PMMA's thickness. Thus, the obtained results supported the agreement which subsequently tended to reduce the Es, since the thickness of the (PMMA/Gr) membrane in this study was approximately 0.5 μm - assuming an effective monolayer graphene thickness of 0.335 nm [8]. The lower value of Es for (PMMA/Gr) membrane supported the idea of contributing to the increased in mechanical sensitivity of the membrane as discussed in the previous section.

IV. CONCLUSION

A hybrid monolayer graphene-PMMA (PMMA/Gr) membrane was fabricated using bulk micromachining and the wet graphene transfer process. The quality of (PMMA/Gr) layer properties was examined using the FESEM and Raman spectroscopy while the mechanical properties of (PMMA/Gr) membrane were determined using nanoindentation testing. From the results of FESEM and Raman, it was shown that the (PMMA/Gr) film had been successfully transferred onto an etched silicon substrate yielding a fully suspended (PMMA/Gr) membrane. The results from the load-displacement curve during the indentation showed that a large displacement was obtained, thus, contributed to a tremendous increase of mechanical sensitivity of the membrane. Through nanoindentation analysis, the (PMMA/Gr) membranes were found to have average tensile stress of 0.58 MPa, which was one of the lowest value from the previous reports for other membrane's material. This resulted in an increment of mechanical sensitivity of the membrane to be approximately of 0.15 nm/Pa, which showed significant improvement, compared to a typical conventional membrane. These results provide some evidence that the (PMMA/Gr) membrane can be a promising material to be applied as a highly sensitive MEMS pressure sensor suited for low pressure sensing detection.

ACKNOWLEDGMENT

The authors would like to acknowledge the Centre for Research and Instrumentation Management (CRIM), UKM, for the FESEM, AFM, and Raman analyses.

REFERENCES

[1] R. Kotsilkova, P. Todorov, E. Ivanov, T. Kaplas, Y. Svirko, A. Paddubskaya, and P. Kuzhir, "Mechanical properties investigation of bilayer graphene/poly(methyl methacrylate) thin films at macro, micro and nanoscale," *Carbon*, vol. 100, pp. 355–366, Apr. 2016.

[2] M. Shokrieh, M. Hosseinkhani, M. Naimi-Jamal, and H. Tourani, "Nanoindentation and nanoscratch investigations on graphene-based nanocomposites," *Polym. Test.*, vol. 32, no. 1, pp. 45–51, Feb. 2013.

[3] C. Berger, R. Phillips, A. Centeno, A. Zurutuza, and A. Vijayaraghavan, "Capacitive pressure sensing with suspended graphene–polymer heterostructure membranes," *Nanoscale*, vol. 9, no. 44, pp. 17439–17449, 2017.

[4] J. Torres, Y. Zhu, P. Liu, S. C. Lim, and M. Yun, "Adhesion energies of 2D graphene and MoS_2 to silicon and metal substrates," *Phys. Status Solidi A*, vol. 215, no. 1, Jan. 2018, Art. no. 1700512.

[5] F. A. Khan, S. Akhtar, D. Almohazey, M. Alomari, S. A. Almofty, I. Badr, and A. Elaissari, "Targeted delivery of poly (methyl methacrylate) particles in colon cancer cells selectively attenuates cancer cell proliferation," *Artif. Cells, Nanomed., Biotechnol.*, vol. 47, no. 1, pp. 1533–1542, Dec. 2019.

[6] T. Ramanathan, A. A. Abdala, S. Stankovich, D. A. Dikin, M. Herrera-Alonso, R. D. Piner, D. H. Adamson, H. C. Schniepp, X. Chen, R. S. Ruoff, S. T. Nguyen, I. A. Aksay, R. K. Prud'Homme, and L. C. Brinson, "Functionalized graphene sheets for polymer nanocomposites," *Nature Nanotechnol.*, vol. 3, no. 6, pp. 327–331, 2008.

[7] B. Das, K. E. Prasad, U. Ramamurty, and C. N. R. Rao, "Nano-indentation studies on polymer matrix composites reinforced by few-layer graphene," *Nanotechnology*, vol. 20, no. 12, p. 125705, 2009.

[8] C. Lee, X. Wei, J. W. Kysar, and J. Hone, "Measurement of the elastic properties and intrinsic strength of monolayer graphene," *Science*, vol. 321, no. 5887, pp. 385–388, Jul. 2008.

[9] G.-H. Lee, R. C. Cooper, S. J. An, S. Lee, A. Van Der Zande, N. Petrone, A. G. Hammerberg, C. Lee, B. Crawford, W. Oliver, J. W. Kysar, and J. Hone, "High-Strength chemical-vapor-deposited graphene and grain boundaries," *Science*, vol. 340, no. 6136, pp. 1073–1076, May 2013.

[10] V. Berry, "Impermeability of graphene and its applications," *Carbon*, vol. 62, pp. 1–10, Oct. 2013.

[11] M. K. Blees, A. W. Barnard, P. A. Rose, S. P. Roberts, K. L. McGill, P. Y. Huang, A. R. Ruyack, J. W. Kevek, B. Kobrin, D. A. Muller, and P. L. McEuen, "Graphene kirigami," *Nature*, vol. 524, no. 7564, pp. 204–207, 2015.

[12] D. G. Papageorgiou, I. A. Kinloch, and R. J. Young, "Mechanical properties of graphene and graphene-based nanocomposites," *Progr. Mater. Sci.*, vol. 90, pp. 75–127, Oct. 2017.

[13] A. Nafari, J. Angenete, K. Svensson, A. Sanz-Velasco, and P. Enoksson, "MEMS sensor for *in situ* TEM-nanoindentation with simultaneous force and current measurements," *J. Micromech. Microeng.*, vol. 20, no. 6, 2010, Art. no. 064017.

[14] Z. Wang *et al.*, "Nanoindentation study of polydimethylsiloxane elastic modulus using berkovich and flat punch tips," *J. Appl. Polym. Sci.*, vol. 132, no. 5, pp. 1–7, 2015.

[15] T. Niu, G. Cao, and C. Xiong, "Indentation behavior of the stiffest membrane mounted on a very compliant substrate: Graphene on PDMS," *Int. J. Solids Struct.*, vols. 132–133, pp. 1–8, Feb. 2018.

[16] J. Chen, X. Guo, Q. Tang, C. Zhuang, J. Liu, S. Wu, and B. D. Beake, "Nanomechanical properties of graphene on poly(ethylene terephthalate) substrate," *Carbon*, vol. 55, pp. 144–150, Apr. 2013.

[17] X. Zhu, Y. Zhao, L. Ma, G. Zhang, W. Ren, X. Peng, N. Hu, L. Rintoul, J. M. Bell, and C. Yan, "Graphene coating makes copper more resistant to plastic deformation," *Compos. Commun.*, vol. 12, pp. 106–111, Apr. 2019.

[18] Y. Zhang and C. Pan, "Measurements of mechanical properties and number of layers of graphene from nano-indentation," *Diamond Rel. Mater.*, vol. 24, pp. 1–5, Apr. 2012.

[19] S.-H. Kang, T.-H. Fang, Z.-H. Hong, and C.-H. Chuang, "Mechanical properties of free-standing graphene oxide," *Diamond Rel. Mater.*, vol. 38, pp. 73–78, Sep. 2013.

[20] N. Yusof, B. Bais, B. Yeop Majlis, N. Soin, and J. Yunas, "Optimization of KOH etching process for MEMS square diaphragm using response surface method," *Indonesian J. Elect. Eng. Comput. Sci.*, vol. 15, no. 1, p. 113, Apr. 2019.

[21] N. Burham, A. A. Hamzah, J. Yunas, and B. Y. Majlis, "Electrochemically etched nanoporous silicon membrane for separation of biological molecules in mixture," *J. Micromech. Microeng.*, vol. 27, no. 7, Jul. 2017, Art. no. 075021.

[22] N. Marsi, B. Y. Majlis, F. Mohd-Yasin, and A. A. Hamzah, "The fabrication of back etching 3C-SiC-on-Si diaphragm employing KOH + IPA in MEMS capacitive pressure sensor," *Microsyst. Technol.*, vol. 21, no. 8, pp. 1651–1661, Aug. 2015.

[23] K. Batrakov, P. Kuzhir, S. Maksimenko, A. Paddubskaya, S. Voronovich, P. Lambin, T. Kaplas, and Y. Svirko, "Flexible transparent graphene/polymer multilayers for efficient electromagnetic field absorption," *Sci. Rep.*, vol. 4, p. 7191, Nov. 2014.

[24] E. Auchter, J. Marquez, S. L. Yarbro, and E. Dervishi, "A facile alternative technique for large-area graphene transfer via sacrificial polymer," *AIP Adv.*, vol. 7, no. 12, Dec. 2017, Art. no. 125306.

[25] F. Kafiah, Z. Khan, A. Ibrahim, M. Atieh, and T. Laoui, "Synthesis of graphene based membranes: effect of substrate surface properties on monolayer graphene transfer," *Materials*, vol. 10, no. 1, p. 86, Jan. 2017.

[26] T. Ondarçuhu, V. Thomas, M. Nuñez, E. Dujardin, A. Rahman, C. T. Black, and A. Checco, "Wettability of partially suspended graphene," *Sci. Rep.*, vol. 6, Apr. 2016, Art. no. 024237.

[27] R. A. Tarefder and H. Faisal, "Effects of dwell time and loading rate on the nanoindentation behavior of asphaltic materials," *J. Nanomech. Micromech.*, vol. 3, no. 2, pp. 17–23, Jun. 2013.

[28] Anthony C. Fischer-Cripps, "Nanoindentation testing," in *Introduction to Contact Mechanics* (Mechanical Engineering Series). New York, NY, USA: Springer, 2000, pp. 20–35.

[29] C. Anthony Fischer-Cripps, "Introduction to contact mechanics," in *Mechanical Engineering Series*, 2nd ed. New York, NY, USA: Springer, 2007, p. 101.

[30] S. A. Zawawi, A. A. Hamzah, B. Y. Majlis, and F. Mohd-Yasin, "Nanoindentation of cubic silicon carbide on silicon film," *Jpn. J. Appl. Phys.*, vol. 58, no. 5, May 2019, Art. no. 051006.

[31] B. J. Briscoe, L. Fiori, and E. Pelillo, "Nano-indentation of polymeric surfaces," *J. Phys. D, Appl. Phys.*, vol. 31, no. 19, pp. 2395–2405, Oct. 1998.

[32] Z. Li, I. A. Kinloch, R. J. Young, K. S. Novoselov, G. Anagnostopoulos, J. P. C. Galiotis, K. Papagelis, C.-Y. Lu, and L. Britnell, "Deformation of wrinkled graphene," *ACS Nano*, vol. 9, no. 4, pp. 3917–3925, 2015.

[33] S. Berciaud, S. Ryu, L. E. Brus, and T. F. Heinz, "Probing the intrinsic properties of exfoliated graphene: Raman spectroscopy of free-standing monolayers," *Nano Lett.*, vol. 9, no. 1, pp. 346–352, Jan. 2009.

[34] A. C. Ferrari, J. C. Meyer, V. Scardaci, C. Casiraghi, M. Lazzeri, F. Mauri, S. Piscanec, D. Jiang, K. S. Novoselov, S. Roth, and A. K. Geim, "Raman spectrum of graphene and graphene layers," *Phys. Rev. Lett.*, vol. 97, no. 18, 2006, Art. no. 187401.

[35] A. C. Ferrari, "Raman spectroscopy of graphene and graphite: Disorder, electron–phonon coupling, doping and nonadiabatic effects," *Solid State Commun.*, vol. 143, nos. 1–2, pp. 47–57, 2007.

[36] V. T. Nguyen, H. D. Le, V. C. Nguyen, T. T. T. Ngo, D. Q. Le, X. N. Nguyen, and N. M. Phan, "Synthesis of multi-layer graphene films on copper tape by atmospheric pressure chemical vapor deposition method," *Adv. Natural Sci., Nanosci. Nanotechnol.*, vol. 4, no. 3, Jun. 2013, Art. no. 035012.

[37] S. Markutsya, C. Jiang, Y. Pikus, and V. V. Tsukruk, "Freely suspended layer-by-layer nanomembranes: Testing micromechanical properties," *Adv. Funct. Mater.*, vol. 15, no. 5, pp. 771–780, May 2005.

[38] B. A. Ganji and B. Y. Majlis, "Design and fabrication of a new MEMS capacitive microphone using a perforated aluminum diaphragm," *Sens. Actuators A, Phys.*, vol. 149, no. 1, pp. 29–37, Jan. 2009.

[39] M. Fu, A. Dehe, and R. Lerch, "Analytical analysis and finite element simulation of advanced membranes for silicon microphones," *IEEE Sensors J.*, vol. 5, no. 5, pp. 857–863, Oct. 2005.

[40] J. Ahmadnejad, B. Azizollahganji, and A. Nemati, "A mems capacitive microphone modelling for integrated circuits," *Int. J. Eng.*, vol. 28, no. 6, pp. 888–895, 2015.

[41] M. S. Nateri and B. A. Ganji, "Design of novel high sensitive mems capacitive fingerprint sensor," *Int. J. Eng.*, vol. 25, no. 3, pp. 167–174, Nov. 2012.

[42] N. Yusof, B. Bais, B. Y. Majlis, and N. Soin, "Mechanical analysis of MEMS diaphragm for bladder pressure monitoring," in *Proc. IEEE Regional Symp. Micro Nanoelectron. (RSM)*, Aug. 2017, pp. 22–25.

[43] Y.-M. Chen, S.-M. He, C.-H. Huang, C.-C. Huang, W.-P. Shih, C.-L. Chu, J. Kong, J. Li, and C.-Y. Su, "Ultra-large suspended graphene as a highly elastic membrane for capacitive pressure sensors," *Nanoscale*, vol. 8, no. 6, pp. 3555–3564, Jan. 2016.
[44] B. A. Ganji, "Design and Fabrication of a Novel MEMS Silicon Microphone," in *Intech*, vol. 2011, pp. 313–328.
[45] S. T. Woo, "Realization of a high sensitivity microphone for a hearing aid using a graphene–PMMA laminated diaphragm," *ACS Appl. Mater. Interfaces*, vol. 9, no. 2, pp. 1237–1246, 2017.
[46] A. Torkkeli, O. Rusanen, J. Saarilahti, H. Seppä, H. Sipola, and J. Hietanen, "Capacitive microphone with low-stress polysilicon membrane and high-stress polysilicon backplate," *Sens. Actuators A, Phys.*, vol. 85, nos. 1–3, pp. 116–123, 2000.
[47] W. Kronast, B. Müller, W. Siedel, and A. Stoffel, "Single-chip condenser microphone using porous silicon as sacrificial layer for the air gap," *Sens. Actuators A, Phys.*, vol. 87, pp. 188–193, Jan. 2001.
[48] K. Lin, Y. Yu, J. Xi, H. Li, Q. Guo, J. Tong, and L. Su, "A fiber-coupled self-mixing laser diode for the measurement of Young's modulus," *Sensors*, vol. 16, no. 6, p. 928, 2016.

BADARIAH BAIS (Senior Member, IEEE) received the B.Sc. degree in electronics engineering and the M.Sc. degree in microelectronics from the Worcester Polytechnic Institute, Worcester, MA, USA, in 1990 and 1992, respectively, and the Ph.D. degree from the Institute of Microengineering and Nanoelectronics (IMEN), Universiti Kebangsaan Malaysia, in 2007. Since 1997, she has been serving at the Department of Electrical, Electronics and Systems Engineering (currently Centre of Advanced Electronic and Communication Engineering (PAKET)), Universiti Kebangsaan Malaysia, as an Academic Staff, where she is currently an Associate Professor. Her research interests include MEMS sensors and microfabrication.

NORLIANA YUSOF received the B.Eng. degree (Hons.) from Universiti Teknologi Malaysia, in 2004, and the M.Eng. degree from the University of Malaya, Malaysia, in 2010. She is currently pursuing the Ph.D. degree with the Institute of Microengineering and Nanoelectronics (IMEN), Universiti Kebangsaan Malaysia, Bangi, Malaysia. Since 2004, she has been serving at the Faculty of Innovative Design and Technology, Universiti Sultan Zainal Abidin, as an Academic Staff. Her current research interests include micro-electro-mechanical systems (MEMS) devices, microfabrication process, and the fundamental study of graphene/polymer membrane.

NORHAYATI SOIN (Senior Member, IEEE) received the B.Eng. (Hons.) and M.Sc. degrees from Liverpool John Moores University, Liverpool, U.K., in 1991 and 1998, respectively, and the Ph.D. degree from the National University of Malaysia, Bangi, Malaysia, in 2006. She is currently a Professor with the University of Malaya, Kuala Lumpur, Malaysia. Her current research interests include micro-electro-mechanical systems (MEMS) devices, microelectronics, and IC design and semiconductor device modeling. She is a Senior Member of the IEEE Electron Devices Society (EDS).

JUMRIL YUNAS received the bachelor's and master's degrees in electrical engineering from RWTH Aachen University, Germany, and the Ph.D. degree in MEMS and nanoelectronics from Universiti Kebangsaan Malaysia (UKM), in 2008. He is currently an Associate Professor with the Institute of Microengineering and Nanoelectronics (IMEN), UKM, Malaysia. His current research interests include MEMS/NEMS devices and technology, lab-on-chip, microsensors and microactuators, RF devices, power electronics, and optoelectronic devices.

BURHANUDDIN YEOP MAJLIS (Senior Member, IEEE) received the B.Sc. degree (Hons.) in physics from UKM, in 1979, the M.Sc. degree in microelectronics from the University of Wales, U.K., in 1980, and the Ph.D. degree in microelectronics from Durham University, U.K., in 1988. His current interests are design and fabrication of MEMS sensor, RF MEMS, BiOMEMS, and microenergy. He is the Chairman of the IEEE Electron Devices Malaysia Chapter, from 1994 to 2006.